Neuron, Vol. 24, 727–737, November, 1999, Copyright ©1999 by Cell Press

Synergistic Release of Ca^{2+} from IP_3-Sensitive Stores Evoked by Synaptic Activation of mGluRs Paired with Backpropagating Action Potentials

Takeshi Nakamura, Jean-Gaël Barbara, Kyoko Nakamura, and William N. Ross*
Department of Physiology
New York Medical College
Valhalla, New York 10595

Summary

Increases in postsynaptic $[Ca^{2+}]_i$ can result from Ca^{2+} entry through ligand-gated channels or voltage-gated Ca^{2+} channels, or through release from intracellular stores. Most attention has focused on entry through the N-methyl-D-aspartate (NMDA) receptor in causing $[Ca^{2+}]_i$ increases since this pathway requires both presynaptic stimulation and postsynaptic depolarization, making it a central component in models of synaptic plasticity. Here, we report that repetitive synaptic activation of metabotropic glutamate receptors (mGluRs), paired with backpropagating action potentials, causes large, wave-like increases in $[Ca^{2+}]_i$ predominantly in restricted regions of the proximal apical dendrites and soma of hippocampal CA1 pyramidal neurons. $[Ca^{2+}]_i$ changes of several micromolars can be reached by regenerative release caused by the synergistic effect of mGluR-generated inositol 1,4,5-trisphosphate (IP_3) and spike-evoked Ca^{2+} entry acting on the IP_3 receptor.

Introduction

Synaptically activated action potentials propagate down the axons and back into the dendrites of hippocampal pyramidal neurons (Turner et al., 1991; Spruston et al., 1995). There has been considerable interest in the backpropagating spikes since they are a message to the cell that both a synaptic input and a postsynaptic response have occurred (for review, see Linden, 1999). This kind of Hebbian interaction is the basis for many models of synaptic plasticity. The form of the message is not clear. An important component is likely to be a rise in postsynaptic $[Ca^{2+}]_i$. Action potentials directly cause $[Ca^{2+}]_i$ increases in the dendrites by opening voltage-sensitive Ca^{2+} channels (Jaffe et al., 1992). There is also evidence that the spikes enhance Ca^{2+} entry through N-methyl-D-aspartate (NMDA) receptor channels (Yuste and Denk, 1995; Koester and Sakmann, 1998; Schiller et al., 1998).

A third pathway for raising $[Ca^{2+}]_i$ is release of Ca^{2+} from intracellular stores. Several studies have suggested that synaptically activated release contributes to the rise of postsynaptic $[Ca^{2+}]_i$ in pyramidal neurons (Alford et al., 1993; Frenguelli et al., 1993; Pozzo-Miller et al., 1996; Emptage et al., 1999; Yeckel et al., 1999) and that this release could participate in the induction of synaptic plasticity and gene expression (Reyes and Stanton, 1996; Wang et al., 1997; Berridge, 1998; Yeckel et al., 1999). More than one mechanism may be involved since there is variation among these experiments concerning the receptors that are activated (NMDA or mGluR [metabotrophic glutamate receptor]), the pathways that participate (Ca^{2+}-induced Ca^{2+} release [CICR] or inositol 1,4,5-trisphosphate [IP_3] receptor–mediated activation), the spatial distribution of the $[Ca^{2+}]_i$ changes that are generated (localized to spines or widespread), and even the importance of this mechanism.

A role for backpropagating action potentials in the Ca^{2+} release process has not been examined. Indeed, many investigators have tried to eliminate voltage-gated Ca^{2+} entry in their experiments to avoid confusion as to the source of Ca^{2+} when measuring $[Ca^{2+}]_i$ increases (see Discussion). A commonly accepted view is that the main function of spikes and Ca^{2+} entry is to supply Ca^{2+} to replenish the stores (Friel and Tsien, 1992; Jaffe and Brown, 1994). However, studies of the IP_3 receptor have noted that a rise in $[Ca^{2+}]_i$ enhances IP_3-mediated release of Ca^{2+} from the endoplasmic reticulum (ER; Iino, 1990; Bezprozvanny et al., 1991; Finch et al., 1991). These observations have led to speculation that a coincident increase in the two intracellular messengers could be an important mechanism triggering the release of Ca^{2+} in neurons (Berridge, 1998). One possible form of this interaction is pairing postsynaptic depolarization, to cause Ca^{2+} entry, with presynaptic activity, to activate metabotropic receptors to release IP_3. To examine this possibility, we used whole-cell recording and high-speed fluorescence imaging of pyramidal neurons in slices from the rat hippocampus. An important step was developing conditions in which synaptic stimulation reliably and repeatably evoked Ca^{2+} release from internal stores. We then examined the mechanism of release, the spatial distribution of the $[Ca^{2+}]_i$ change, and the role of action potentials in this process. We found that following synaptic activation, a single spike could trigger regenerative release from IP_3-sensitive stores, which raised $[Ca^{2+}]_i$ several micromolars in the proximal apical dendrites.

Results

To isolate the contribution of mGluRs, we stimulated the slice in the presence of 10 μM 6-cyano-7-nitroquinoxaline-2,3-dione (CNQX) and 100 μM (±)-2-amino-5-phosphonopentanoic acid (AP-5) to block ionotropic glutamate receptors. The sharp point of the stimulating electrode was placed near the proximal apical dendrites of the bis-fura-2-filled pyramidal neuron (Figure 1B). Under these conditions, stimulation at 100 Hz for 0.25–1.0 s caused a slow depolarization of the membrane (Figure 1C, bottom). The depolarization usually was preceded by a brief hyperpolarization that was caused by coactivation of inhibitory inputs which were not blocked in these experiments (e.g., Figures 1D, 2A, and 5A). In many cells ($n = 24$), this stimulation caused a transient increase in $[Ca^{2+}]_i$ that began with a delay (Figure 1C). The shortest observed delay from the beginning of stimulation was 0.4 s and the longest, 1.3 s (mean 0.72 ±

*To whom correspondence should be addressed (e-mail: ross@nymc.edu).

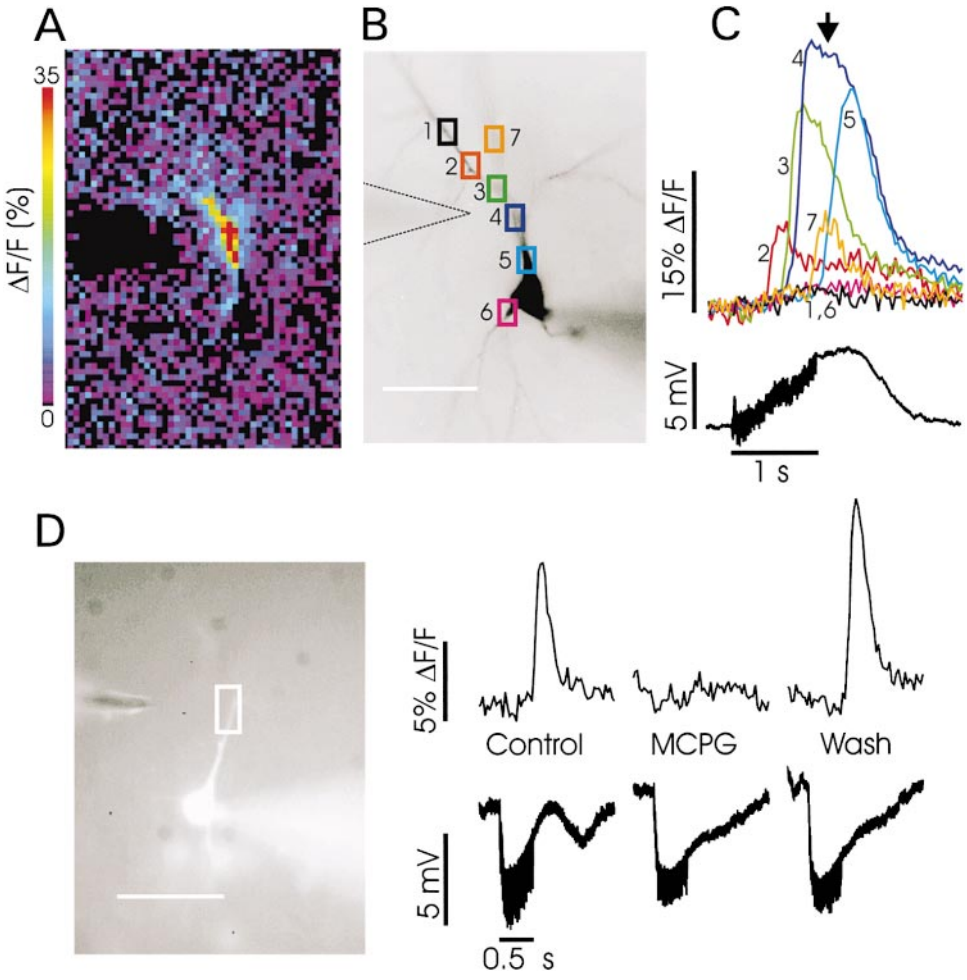

Figure 1. Repetitive Synaptic Stimulation Causes Localized Ca^{2+} Waves in Pyramidal Cell Dendrites

(A) Pseudocolor image of the restricted spatial distribution of the amplitudes of the fluorescence changes at the time indicated by the vertical arrow over the fluorescence traces in (C). The image is matched to the cell image in (B).

(B) Fluorescence image of a pyramidal cell filled with bis-fura-2. The patch electrode used for intracellular stimulation and recording is visible. The position of the extracellular stimulating electrode is indicated by a dotted line. Scale bar, 50 μm.

(C) Time-dependent fluorescence changes measured at different dendritic locations (indicated by rectangles in [B]) and somatic membrane potential change in response to 100 Hz synaptic stimulation for 1 s. AP-5 (100 μM) and CNQX (10 μM) were added to the ACSF. The fluorescence changes began near location 2 and propagated to location 5. From location 4, the wave backpropagated for a short distance into another dendrite (location 7). There was no detectable increase at locations 1 and 6, which border this region. The fluorescence increase at even the earliest location (2) was delayed by about 0.5 s from the start of synaptic stimulation.

(D) In another cell, 100 Hz synaptic stimulation for 0.5 s caused a delayed $[Ca^{2+}]_i$ increase at the indicated location near the stimulating electrode. This increase was reversibly blocked by 1 mM MCPG.

0.27 s, n = 23 cells). Transients as short as 200 ms were measured in the dendrites (mean 0.48 ± 0.18 s, n = 23) but could last more than 1.5 s in the soma if they invaded that region. Multiple stimuli (usually 25) were required to observe this $[Ca^{2+}]_i$ increase, but we did not try to determine the threshold stimulation configuration. The $[Ca^{2+}]_i$ increase was not synchronous at all locations; the peak spread as a wave over a restricted region near the point of stimulation (Figure 1C; to see a movie of this wave, go to http://www.neuron.org/cgi/content/full/24/3/727/DC1). Examples of propagation in one or both directions were observed. Typical propagation velocities were 68 ± 22 μm/s (n = 18) but were not constant along a dendrite. Transients could be evoked repeatedly in the same neuron. These Ca^{2+} transients required action potential-mediated release of neurotransmitter since they were blocked by tetrodotoxin (TTX, 1 μM) when the postsynaptic responses were subthreshold (n = 2; data not shown). To confirm that the release in our experiments was due to activation of mGluR, we applied (R,S)-α-methyl-4-carboxyphenylglycine (MCPG, 1 mM; n = 2; Conn and Pin, 1997), which reversibly blocked the slow Ca^{2+} transients (Figure 1D). As MCPG was added to the preparation, the spatial extent of the release wave became more restricted before being eliminated. MCPG also blocked the slow membrane depolarization, consistent with previous observations (Davies et al., 1995; Congar et al., 1997).

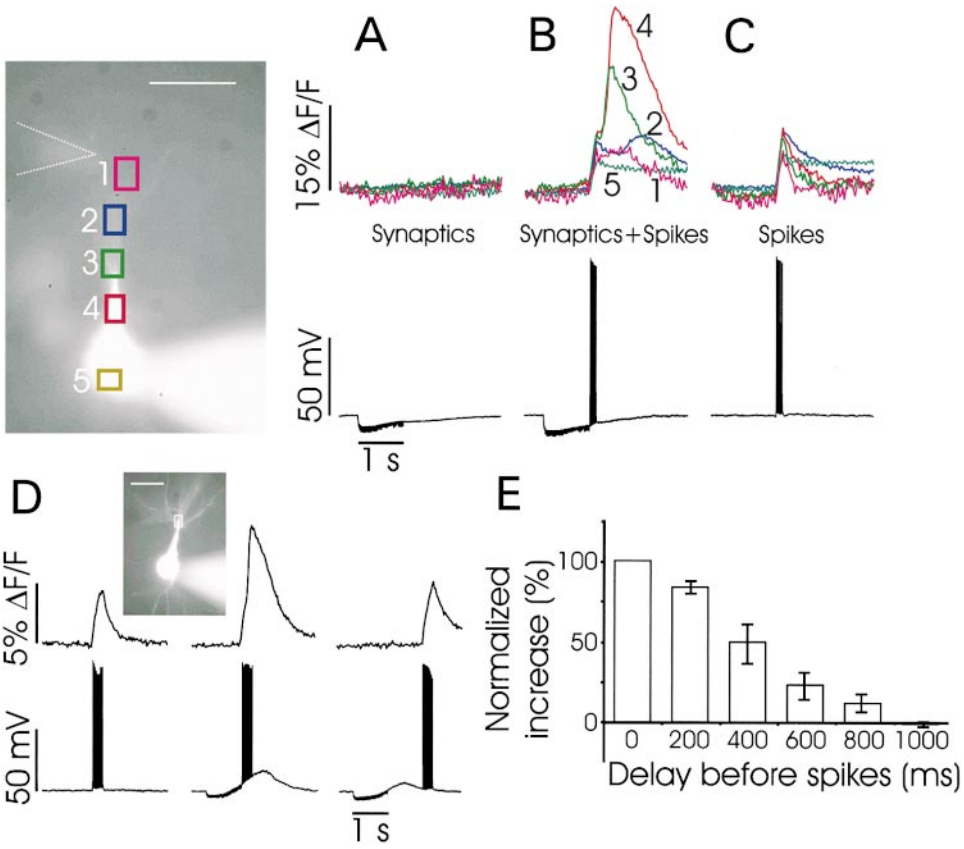

Figure 2. Synaptic Stimulation followed by Action Potentials Causes Release of Ca^{2+} in the Apical Dendrites

Left panel shows bis-fura-2-filled pyramidal neuron, with regions of interest and electrode positions marked. AP-5 (100 μM) and CNQX (10 μM) were added to the ACSF. Scale bar, 50 μm.

(A) Synaptic stimulation at 100 Hz for 1 s caused no detectable change in fluorescence at any somatic or dendritic location. The membrane potential hyperpolarized because inhibition was not blocked.

(B) Synaptic stimulation (same stimulation parameters) followed immediately by action potentials, evoked by 1 ms intrasomatic pulses at 30 ms intervals, caused fast fluorescence increases at all locations and slower, larger increases, predominantly in the proximal apical dendrites.

(C) A train of ten action potentials without synaptic stimulation evoked fluorescence increases that peaked at the time of the last spike at all locations.

(D) A similar experiment in another cell. Fluorescence changes measured from the rectangular region are indicated in the inset. The first panel shows a fast fluorescence increase in response to ten action potentials stimulated at 30 ms intervals. The second panel shows a larger, regenerative increase when the spikes were immediately preceded by synaptic stimulation (100 Hz for 1 s). The last panel shows a smaller, faster increase when the spikes were delayed by 1 s.

(E) Increase in amplitude of the fluorescence change versus time of delay of spikes after the end of synaptic stimulation. Increases normalized to 100% at zero delay. Nine cells are included in the histogram. Not all times were measured for each cell.

Weaker stimulation and more distal stimulation also were effective in inducing a hyperpolarization followed by a depolarization. However, in many cells ($n = 46$), stimulation under these conditions caused no change in $[Ca^{2+}]_i$ (Figure 2A). In these experiments, we could usually cause large $[Ca^{2+}]_i$ increases if we followed the synaptic stimulation with a short train of action potentials (typically five to ten spikes at 30 ms intervals) evoked with brief current pulses in the soma (Figure 2B). These increases had a sharp initial phase that correlated with the spikes and a slower, secondary phase. The secondary increases were not synchronous in all of the dendritic locations where they were observed. However, they were more synchronous than those of the propagating waves observed without spikes. This pattern was clearly different from the temporal profile of $[Ca^{2+}]_i$ changes caused by action potentials alone (Figure 2C). These nonsynaptic, spike-evoked $[Ca^{2+}]_i$ changes peaked simultaneously at all locations (within one frame interval) at the time of the last action potential. The delayed increase, induced by synaptic stimulation and action potentials, like the increases observed without spikes, could be blocked by 1 mM MCPG ($n = 8$; data not shown). MCPG had no effect on the $[Ca^{2+}]_i$ transients evoked by spikes alone. The enhanced release also was observed in cells in which spikes were generated by excitatory postsynaptic potentials (EPSPs) in experiments that did not include AP-5 and CNQX in the artificial cerebrospinal fluid (ACSF; data not shown).

When the spikes were evoked immediately at the end of the synaptic train, they usually caused a Ca^{2+} release transient in the dendrites. However, in the same cells

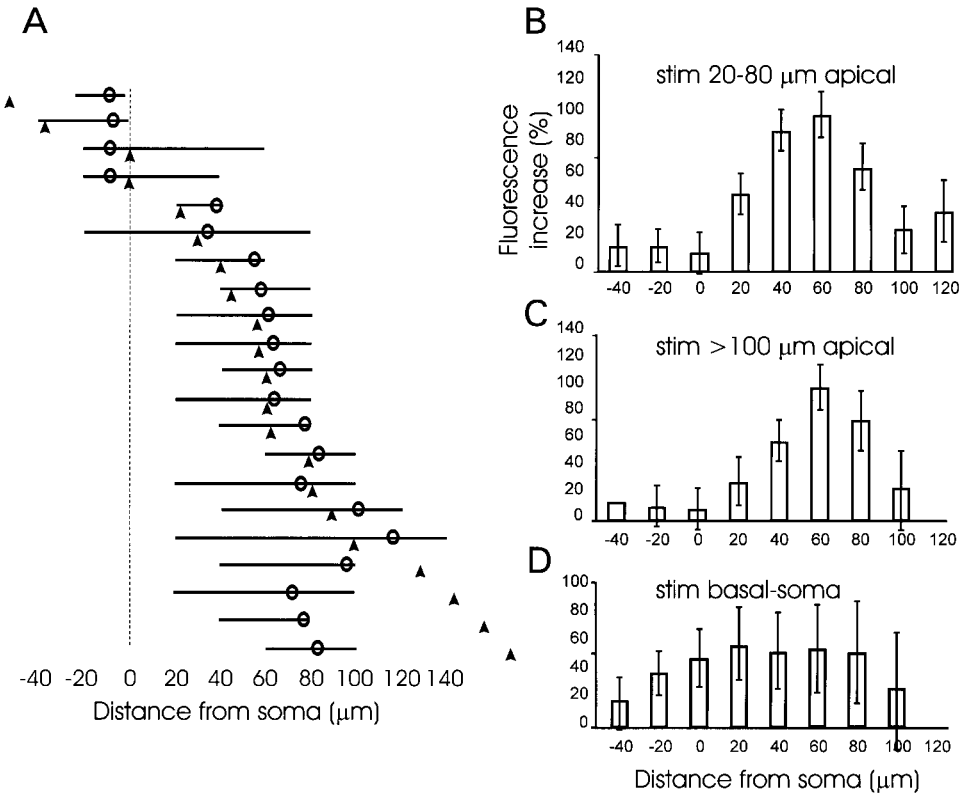

Figure 3. Spatial Distribution of Synaptically Evoked Ca^{2+} Release

(A) Distribution of $[Ca^{2+}]_i$ increases in cells in which spikes were not needed to cause release. Each line is from a different cell. The length and position of the line indicate where release was detected (to the nearest 20 μm). The arrowhead indicates the position of the stimulating electrode. The circle indicates the location where release was first detected. In the proximal apical region, release occurred near the site of stimulation. Stimulation outside this region either was not effective or preferentially caused release in the proximal apical region or soma.

(B) Spatial distribution in cells in which a train of 20 spikes was used to evoke release following synaptic stimulation in the proximal apical dendrites (20–80 μm from the soma). At each location, the ratio of the fluorescence increase with both synaptic stimulation and spikes is compared with the increase when spikes alone were stimulated. Data from twenty-three cells are included in the histogram. The largest increase was in the proximal apical region.

(C) Similar histogram for nine cells in which the stimulating electrode was placed more than 100 μm from the soma.

(D) Distribution of increases for six cells when the stimulating electrode was positioned at the soma to 40 μm into the basal dendrites. Stimulation in this region often did not generate release, using currents that were effective in the apical dendrites. Higher stimulating currents evoked antidromic action potentials.

no release was observed when the spikes were evoked 1 s after the end of the train (Figure 2D). Similarly, release transients were not detected when spikes were evoked at the beginning of tetanic synaptic stimulation (data not shown). Figure 2E shows a summary histogram of nine similar timing experiments. For each cell, the interval between the end of synaptic stimulation and the beginning of spike stimulation was varied, and the magnitude of release was noted. The figure shows that the fractional increase in amplitude of the release transient (normalized to the increase at zero delay) rapidly declined as the interval before spike stimulation increased to 1 s.

Localized release without spikes was observed most commonly when the stimulating electrode was placed close to the base of the proximal apical dendrites. In these experiments, release appeared to begin at a location near the electrode tip and then propagated for variable distances, but rarely more than 50 μm from the initiation point. If the electrode was close to the soma, initiation occurred close to the soma, and the wave propagated toward the dendrites. If initiation was away from the soma, then propagation was toward the soma. In most cases, the wave was confined to the proximal apical region of the dendrites. In some cells, the wave spread over the soma. In several cells, the wave continued into the basal dendrites, but with reduced amplitude and rarely more than 20 μm from the soma. If stimulation was outside the sensitive region (soma to ~100 μm into the apical dendrites), then higher current densities were usually required to evoke release. However, in these cases the release waves were still predominantly in the proximal apical region or soma. These patterns are summarized in Figure 3A.

When spikes were used to evoke release after synaptic stimulation, the $[Ca^{2+}]_i$ increase due to release was also concentrated in the proximal apical dendrites, although it appeared to extend over a slightly larger area than release evoked without spikes. In contrast, the spike-evoked $[Ca^{2+}]_i$ increase in normal ACSF could be

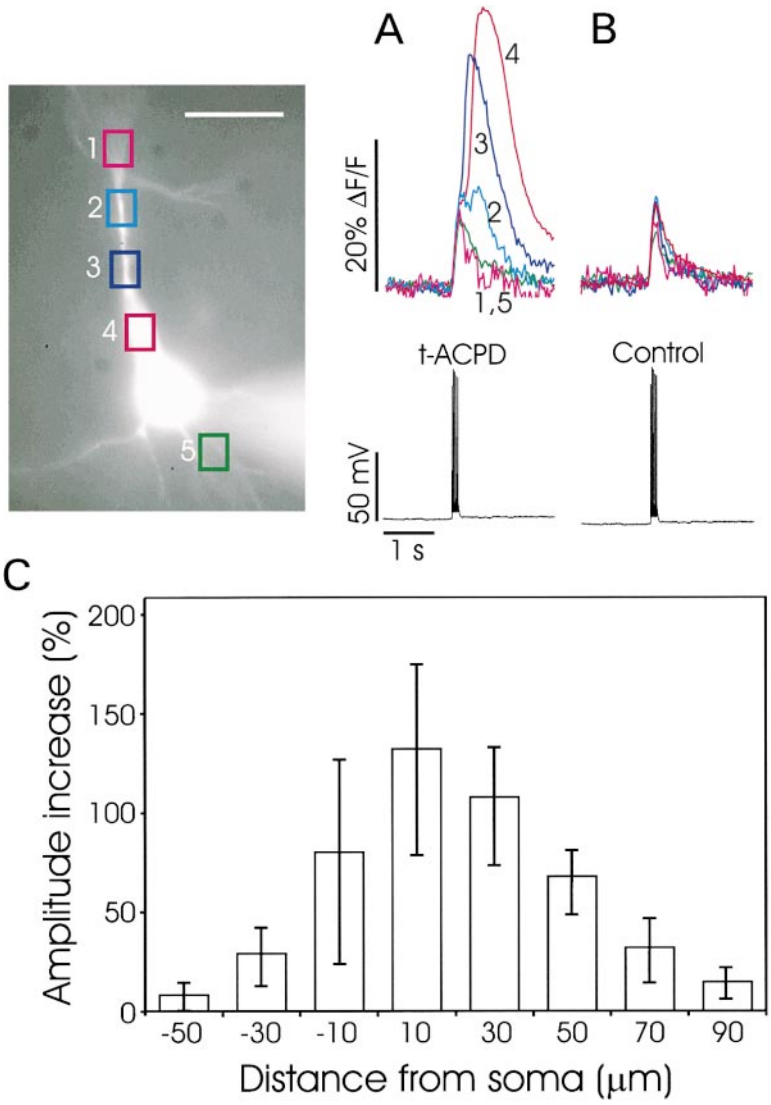

Figure 4. Spikes Cause Ca^{2+} Release in the Proximal Apical Dendrites in the Presence of t-ACPD

Left panel shows a pyramidal neuron filled with bis-fura-2, with regions of interest indicated. AP-5 (100 μM) and CNQX (10 μM) were always present. Scale bar, 50 μm.

(A) In ACSF containing 30 μM t-ACPD, a train of five intrasomatically evoked action potentials (30 ms intervals) generated a fast fluorescence increase at all locations (1–5) followed by a slower increase at locations 2–4 in the proximal apical dendrites.

(B) The same action potentials generated only fast fluorescence changes in normal ACSF.

(C) Spatial distribution of the amplitude increase in t-ACPD compared with the amplitude in normal ACSF. Data from nine cells are included in the histogram. All cells showed increases in the apical dendrites (30–50 μm). Only six of these showed increases in the soma (−10, 10 μm). However, these increases were large, explaining the bigger error bars at these locations.

observed out to the limits of the apical and basal dendrites or at least as far as fluorescence could be detected (Jaffe et al., 1992; Callaway and Ross, 1995; Spruston et al., 1995). To determine more quantitatively the spatial distribution of release in these experiments, we calculated at each location the percentage increase in the fluorescence change when spikes followed synaptic stimulation compared with the change evoked by spikes alone. Data were separated into three groups, depending on the location of the stimulating electrode. Figure 3B shows the distribution when stimulation was in the proximal apical dendrites. In this case, the greatest increase was near the stimulating electrode. In nine cells in which the stimulating electrode was placed more apical to the sensitive region (>100 μm), release evoked by spikes was still largest in the same proximal apical region (Figure 3C). Even when the stimulating electrode was placed near the soma or on the basal dendrites, the largest increases were in the apical dendrites (Figure 3D).

It was clear from these experiments that it was harder to evoke release when the stimulating electrode was positioned more distally in the apical dendrites or over the basal dendrites. This would seem to suggest that the synapses in these regions were less capable of inducing release than those in the proximal apical dendrites. However, the dendrites in these other regions are thinner and more branched than the dendrites in the sensitive proximal apical region. In addition, the spatial organization of fibers stimulated by the tungsten electrode was not exactly known. Therefore, extracellular synaptic stimulation might not be equally effective in all regions of the pyramidal neuron. One possible way of dealing with this problem is to activate all mGluRs equally with an exogenously applied agonist. To this end, 30 μM trans-1-amino-cyclopentyl-1,3-dicarboxylate (t-ACPD, an mGluR agonist; Conn and Pin, 1997) was added to the bath. The cell depolarized by about 5 mV, and there was a small or no change in resting $[Ca^{2+}]_i$, as judged by the fluorescence intensity in the soma and proximal dendrites (Davies et al., 1995; Bianchi et al., 1999). When a train of action potentials was evoked with intrasomatic stimulation, large regenerative $[Ca^{2+}]_i$ changes were detected, predominantly in the proximal apical dendrites

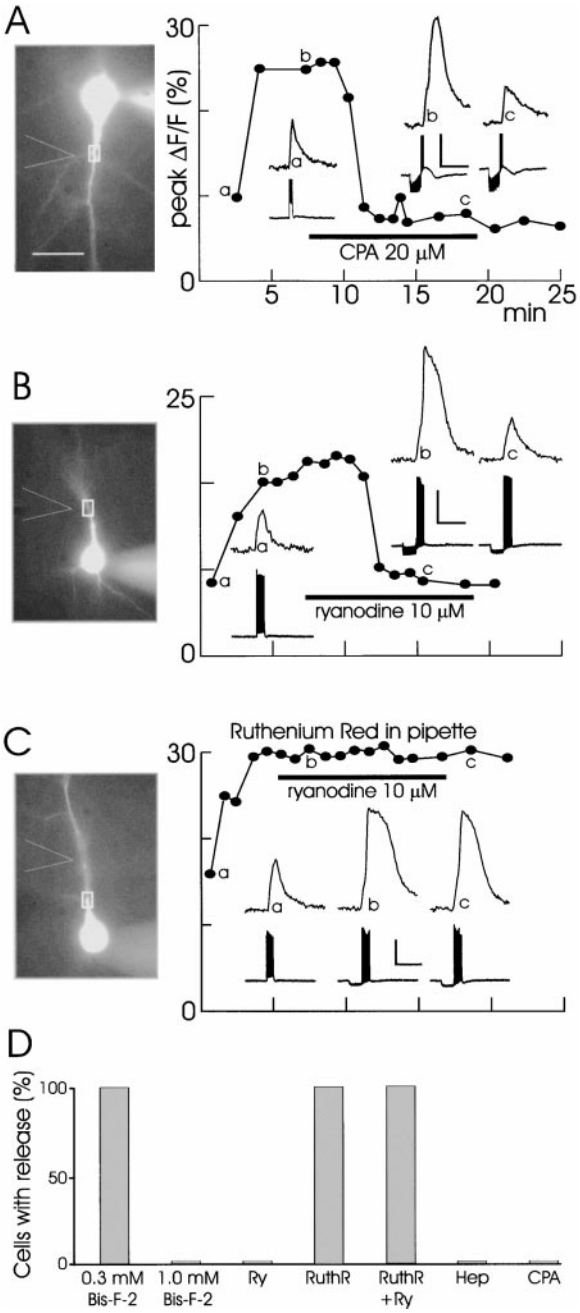

Figure 5. Pharmacology of Synaptically Evoked Ca^{2+} Release

(A) Effect of 20 μM CPA. Left panel shows a bis-fura-2-filled pyramidal neuron, with electrode positions and region of interest indicated. In the first trial (a), five spikes alone at 30 ms intervals generated a small fluorescence increase that was linked in time to the spikes (left inset, [a]). Subsequent trials used synaptic stimulation (100 Hz for 500 ms) followed by the same train of action potentials. This protocol evoked a regenerative fluorescence increase in the apical dendrites that outlasted the spikes (middle inset, [b]). Following superfusion with 20 μM CPA, the regenerative increase was blocked, leaving an increase of about the same amplitude as that generated by spikes alone (right inset, [c]). The segmented line shows the peak fluorescence amplitude for all trials during the 25 min experiment. Note that the IPSP and the slow depolarization under the spikes remained. Peaks of action potentials in all panels have been cut off to show the synaptic responses in more detail. Scale: ordinate, 10 mV and 10% ΔF/F; abscissa, 1 s. Scale bar, 50 μm.

(B) Similar experiment showing that 10 μM ryanodine blocked synaptically evoked release. Same scales, except that ordinate for voltage is 75 mV.

(C) Similar experiment showing that 10 μM ryanodine did not block release when the cell was loaded from a pipette containing 120 μM Ruthenium Red.

(D) Summary of effects of different agents on the ability of synaptic stimulation and spikes to evoke release. Cells were scored as positive if the stimulated fluorescence increase was significantly larger than the increase due to spikes alone. Abscissa labels indicate the additions to the pipette and ACSF solutions used in these experiments: 0.3 mM Bis-F-2 (bis-fura-2, 0.3 mM in pipette; $n > 50$) is the control condition; 1.0 mM Bis-F-2 ($n = 5$); Ry (ryanodine, 10–40 μM added to ACSF; $n = 12$); RuthR (Ruthenium Red, 80–120 μM in pipette; $n = 10$); RuthR + Ry (Ruthenium Red, 120 μM in pipette; ryanodine, 10 μM in ACSF; $n = 3$); Hep (heparin, 1 mg/ml in pipette; $n = 5$); and CPA (20 μM in ACSF; $n = 6$).

($n > 30$; Figure 4A). These changes were larger and longer lasting than the transients evoked by spikes without t-ACPD in the bath (Figure 4B) and resembled the regenerative $[Ca^{2+}]_i$ changes evoked by action potentials following synaptic stimulation (Figure 2B). Figure 4C shows the spatial distribution of the increase determined from an analysis of nine cells. It is clear that, as with the synaptically evoked transients, the enhancement was most dramatic in the proximal apical dendrites and soma.

Several pharmacological experiments support the conclusion that the regenerative increase in $[Ca^{2+}]_i$ is due to the synergistic action of IP_3 and Ca^{2+} acting on the IP_3 receptor to release Ca^{2+} from intracellular stores. First, synaptically evoked release was blocked by 20 μM cyclopiazonic acid (CPA; $n = 6$; Figure 5A), which depletes intracellular stores by blocking the ER Ca^{2+}-ATPase (Seidler et al., 1989). CPA did not prevent the release of neurotransmitter since the inhibitory postsynaptic potential (IPSP) and slow EPSP were still recorded (Figure 5A, insets). Further evidence that CPA acted postsynaptically is that it prevented the slow, spike-evoked release in the presence of 30 μM t-ACPD ($n = 7$; data not shown). CPA had little effect on the spike-evoked $[Ca^{2+}]_i$ increase in normal ACSF, consistent with entry through voltage-sensitive channels as the primary pathway for this $[Ca^{2+}]_i$ change (Markram et al., 1995). Second, release was prevented by including low-molecular weight heparin (1 mg/ml; $n = 5$) in the pipette. Heparin blocks the binding of IP_3 to its receptors in neurons and other cell types and prevents Ca^{2+} release (Ghosh et al., 1988; Kobayashi et al., 1988). Group I mGluR1s, which are prominently expressed on CA1 pyramidal neurons and which are blocked by MCPG, stimulate IP_3 production when activated (Conn and Pin, 1997). Heparin did not block the slow membrane depolarization, indicating that some of this depolarization is a non-IP_3-mediated consequence of mGluR activation (data not shown).

The large $[Ca^{2+}]_i$ increase caused by backpropagating action potentials suggests that the spikes might participate in the release process by transiently raising $[Ca^{2+}]_i$ above a threshold level. To test this idea, we increased the bis-fura-2 concentration to 1 mM in the recording pipette to buffer the spike-evoked transients. Indeed, as previously reported (e.g., Helmchen et al., 1996), the

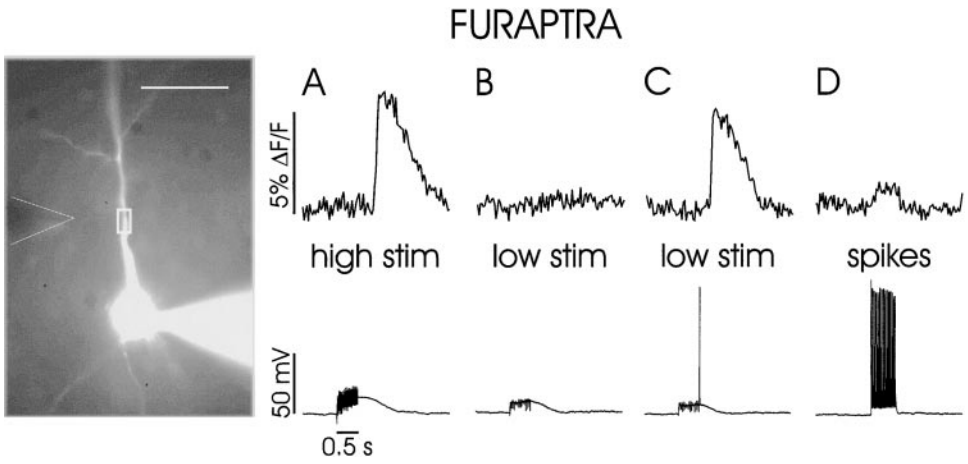

Figure 6. Synaptically Evoked and Spike-Evoked Ca^{2+} Release Measured with the Low-Affinity Indicator Furaptra

The image shows a pyramidal neuron filled with 500 μM furaptra. The region of interest and the position of the stimulating electrode are indicated. Scale bar, 50 μm.

(A) Response to 50 stimuli at 100 Hz, using 40 μA pulses ("high stim"). This stimulation generated a furaptra fluorescence change >5% in the dendrite.

(B) In response to 30 μA current pulses ("low stim"), no release transient was generated.

(C) The same synaptic stimulation followed by a single intrasomatically evoked action potential generated a large release transient.

(D) Twenty action potentials at 30 ms intervals evoked intrasomatically without synaptic stimulation ("spikes") generated a relatively small fluorescence increase.

$[Ca^{2+}]_i$ increases due to spikes alone were smaller and slower than those measured with 0.3 mM indicator but were clearly visible. In contrast, we found that synaptically evoked release with or without spikes did not occur when 1 mM bis-fura-2 was included in the pipette (n = 5; data not shown), although release was reliably evoked with 0.3 mM bis-fura-2. Since non-spike-evoked release also was prevented by high-bis-fura-2 concentrations, Ca^{2+} is probably an important cofactor for this form of release as well. In this case, it is not clear whether the high-bis-fura-2 concentration is buffering resting $[Ca^{2+}]_i$ below threshold levels or buffering the released Ca^{2+} that contributes to the regenerative $[Ca^{2+}]_i$ increase.

Ca^{2+} could participate in the release process by activating the ryanodine receptor and inducing CICR. This form of regenerative release is known to be important in some peripheral neurons (Friel and Tsien, 1992; Usachev and Thayer, 1997). Indeed, we found that 10 μM (n = 3) or 40 μM ryanodine (n = 9), which depletes stores by blocking the ryanodine receptor in the open state (Rousseau et al., 1987), rapidly prevented synaptically mediated release when added to the ACSF (Figure 5B). However, we found that Ruthenium Red (80–120 μM in the pipette), which blocks the ryanodine receptor in the closed state (Smith et al., 1988) and which at 20 μM blocks CICR in Purkinje cells (Llano et al., 1994), did not prevent synaptically evoked release (n = 10; Figure 5C). To confirm that Ruthenium Red really was blocking the ryanodine receptor, we added ryanodine (10 μM) to the ACSF in preparations in which the pyramidal neurons were loaded with 120 μM Ruthenium Red. In these experiments, release still occurred in the presence of ryanodine (n = 3; Figure 5C). Figure 5D summarizes these pharmacological experiments. Together, these results suggest that the ryanodine-sensitive store communicates with the IP_3-sensitive store (Seymour-Laurent and Barish, 1995), but ryanodine receptor activation does not contribute significantly to the release observed here. This release is primarily mediated by the IP_3 receptor. A similar conclusion was reached for release evoked by activation of caged IP_3 in cerebellar Purkinje cells (Khodakhah and Armstrong, 1997).

The complete inhibition of release by 1 mM bis-fura-2 in the patch pipette suggested that the 0.3 mM indicator used in most of our experiments might buffer $[Ca^{2+}]_i$, affecting the release parameters without blocking release. In addition, since bis-fura-2 is a relatively high-affinity indicator ($K_d \approx 370$ nM), the fluorescence changes evoked by release might be close to saturation. In this case, the fluorescence change would not accurately follow the $[Ca^{2+}]_i$ change. To avoid these problems, we repeated some experiments using the low-affinity indicator furaptra (also known as mag-fura-2). Qualitatively, the responses, using this indicator, were similar to those detected using bis-fura-2 (n = 6). Release transients were detected in response to repetitive synaptic stimulation alone (Figure 6A) and were induced by spikes (Figure 6C) when synaptic stimulation did not evoke a response (Figure 6B). Release was detected primarily in the proximal apical dendrites and propagated as a wave in this region. However, there were some differences. With bis-fura-2 in the pipette, we usually (one exception) needed several action potentials to cause release. With furaptra in the pipette, a single spike was often effective (n = 4/5; Figure 6C). The rate of rise of the release transient at the fastest location was significantly faster (63 ± 4 ms, 10%–90% of peak, n = 6, mean ± SEM) with furaptra than with bis-fura-2 (93 ± 6 ms, n = 10, $p < 0.005$, Student's t test), although the frame rate of the camera reduced the precision of the measurements. Both of these differences can be explained by the lower buffering power of furaptra. In the first case, the spike-evoked $[Ca^{2+}]_i$ increase reaches higher levels with less

buffering and will be more effective in activating the IP_3 receptor. In the second case, more of the released Ca^{2+} binds to IP_3 receptors, accelerating regenerative release (Iino and Endo, 1992).

The magnitude of the furaptra fluorescence increase ranged from 5% to 15% at the site of the largest increase in the dendrites (n = 6). In contrast, the fluorescence increase generated by a train of 20 intrasomatically evoked action potentials was about 1% (n = 5; Figure 6D). Therefore, in conditions with minimum buffering and in which the response of the indicator is linear, the fluorescence change and hence the $[Ca^{2+}]_i$ change caused by release was 5 to 15 times larger than that evoked by a train of action potentials. The ratio is probably even higher in the center of the dendritic shaft or soma since the spike-evoked $[Ca^{2+}]_i$ increase is highest just under the membrane, while that due to release is more uniform.

We can estimate the magnitude of the $[Ca^{2+}]_i$ increase from the fluorescence change since $\Delta[Ca^{2+}]_i \approx K_d \cdot (\Delta F/F)/(\Delta F/F)_{MAX}$ if $(\Delta F/F)/(\Delta F/F)_{MAX} << 1$ (Lev-Ram et al., 1992). From the spectral properties of furaptra, we estimate that $(\Delta F/F)_{MAX} \approx 0.8$ at 380 nm (Konishi et al., 1991), with a maximum possible value of this parameter of 1.0. Using K_d = 36–44 μM for furaptra (Konishi et al., 1991; Naraghi, 1997), our results suggest that the plateau $[Ca^{2+}]_i$ change generated by the spike train is about 400 nM, consistent with measurements made with very low-fura-2 concentrations (Helmchen et al., 1996). The larger synaptically evoked release generated $[Ca^{2+}]_i$ increases of 2–6 μM.

Discussion

These experiments show that synaptic stimulation reliably evokes increases in $[Ca^{2+}]_i$ due to release from intracellular stores. These increases are much larger than $[Ca^{2+}]_i$ changes due to action potentials evoked without synaptic stimulation and can reach amplitudes of several micromolars. They propagate as a wave in restricted regions of hippocampal pyramidal neurons and are due to activation of mGluR and the subsequent generation of IP_3. These transients were observed in essentially 100% of more than 100 cells tested if several conditions were met. These include (1) placement of the stimulating electrode close to the proximal apical dendrite, (2) application of multiple synaptic stimuli, (3) generation of a short train of action potentials within 0.5 s of the synaptic burst, and (4) use of low concentrations of Ca^{2+} indicator or low-affinity indicators. Not all of these conditions were always required. In many cells, action potentials were not necessary if the stimulating electrode was optimally positioned and the stimulation intensity and frequency were adjusted. However, even in these cells action potentials in conjunction with synaptic stimulation would cause release when the stimulation parameters or electrode position was adjusted to be subthreshold for release by synaptic stimulation alone. This result is important because a weaker or more diffuse stimulation protocol is likely to correspond more closely to physiological activation of pyramidal neurons.

Relationship to Previous Experiments

There are some differences between our results and the recently reported synaptically evoked Ca^{2+} release transients in pyramidal cell dendritic spines (Emptage et al., 1999). In those experiments, release depended on NMDA receptor activation and was attributed to CICR. NMDA receptors were blocked in our experiments; release required activation of mGluR. CICR was not significant compared with IP_3-mediated release in our experiments, although we cannot rule out a small contribution via this pathway. One possibility is that the localized release in spines occurs through a different mechanism than the IP_3-mediated Ca^{2+} waves we observed in the dendritic shaft. This would be consistent with the reported presence of ryanodine receptors and absence of IP_3 receptors in pyramidal cell spines (Sharp et al., 1993).

The Ca^{2+} waves observed without spikes in these experiments (Figure 1) resemble the waves previously observed in these cells following the puffing of t-ACPD onto pyramidal cell dendrites (Jaffe and Brown, 1994). They also have characteristics similar to the localized release recently described in Purkinje cells (Finch and Augustine, 1998; Takechi et al., 1998). In those experiments and ours, release was mediated by IP_3 following mGluR activation, required multiple synaptic stimuli, appeared after a delay, and had similar time courses. There are some differences. The release observed in our experiments was most prominent in the thick dendrites near the soma and usually occurred as a wave. In Purkinje cells, release was observed at the spines and at the tips of the fine dendrites, consistent with the high density of IP_3 receptors at those locations in Purkinje cells (Walton et al., 1991). Wavelike release was not described. In addition, no role for voltage-gated Ca^{2+} entry was suggested. Whether these differences signify meaningful mechanistic differences is still to be determined.

Our results also offer possible explanations as to why in some previous experiments it was difficult to evoke release and why in others release was not observed at all. First, in an effort to avoid confusion as to the source of Ca^{2+}, some investigators eliminated or reduced spikes and/or voltage-dependent Ca^{2+} entry by giving subthreshold stimulation (Emptage et al., 1999), washing out Ca^{2+} channels (Alford et al., 1993; Frenguelli et al., 1993), or blocking some Ca^{2+} channels and depolarizing the postsynaptic membrane potential beyond the Ca^{2+} reversal potential (Pozzo-Miller et al., 1996). These procedures would prevent the synergistic effect that Ca^{2+} entry has on the release process. Second, in many early experiments (e.g., Regehr and Tank, 1990; Miyakawa et al., 1992) cells were filled with 2–15 mM fura-2, a higher affinity indicator than bis-fura-2. While the cells were filled from sharp electrodes, making it difficult to know the final concentration in the dendrites, it is likely that these indicator concentrations were higher than the levels that completely suppressed release in our experiments.

Spatial Distribution

Two aspects of the spatial extent of the Ca^{2+} release transients are interesting. First, synaptically evoked release without spikes extended over a distance of about

50 μm (Figure 3A). This distance probably reflects both the spatial extent of the bundle of activated presynaptic fibers and the diffusion of IP_3 from the site of synthesis. The extent of spike-evoked Ca^{2+} entry was not critical since the release transients extended over a similar length when synaptic activation and action potentials were needed to evoke release (Figures 2B and 3B–3D). Second, we found that release transients could be evoked easily only when the stimulating electrode was placed close to the proximal apical dendrites and that, once evoked, they spread as a wave predominantly within this region. A similar spatial distribution for spike-evoked regenerative release was found following bath application of t-ACPD, which activated mGluR at all locations on the pyramidal neurons. The reasons for this restricted distribution are not clear. It is possible that we only detected regenerative release and that more elementary, nonregenerative events ("puffs"; Koizumi et al., 1999) were below the detection threshold in our experiments and were more widely distributed. Even if this explanation were correct, it would still require an explanation for the restricted distribution of regenerative events. mGluRs are widely distributed on pyramidal neurons (Lujan et al., 1996). If this distribution is roughly uniform, then synaptic stimulation should activate the receptors at all locations. However, other molecules participate in the synthesis of IP_3, and their distribution within pyramidal neurons is not known. Therefore, the ability to synthesize IP_3 may not be uniform in these cells. Similarly, the distribution and density of IP_3 receptors are not accurately known. There is evidence that this receptor is concentrated in the proximal apical dendrites of cortical pyramidal neurons (Sharp et al., 1993), but the quantitative distribution in hippocampal cells has not been reported.

Significance of Action Potentials

An important observation in our experiments is that action potentials evoked in a time window following synaptic stimulation could cause release even when synaptic stimulation alone did not cause detectable release. One spike was usually sufficient in conditions of minimal Ca^{2+} buffering. The most likely explanation for this effect, as suggested above, is that the Ca^{2+} entering through voltage-gated Ca^{2+} channels acts synergistically with synaptically generated IP_3 to modulate the IP_3 receptors (Iino, 1990; Bezprozvanny et al., 1991; Finch et al., 1991). Some Ca^{2+} may be required to evoke release even without spikes since high-bis-fura-2 concentrations buffered $[Ca^{2+}]_i$ and prevented this form of release. However, the higher $[Ca^{2+}]_i$ achieved following spike activity makes it easier to open the IP_3 receptor channels. In particular, according to the coactivation model of IP_3 receptor activation, a lower concentration of IP_3 would be needed to open the receptor channels when sufficient Ca^{2+} is present. This would explain why spikes following synaptic activation evoke release even when synaptic activation alone does not.

Release, when detected, was clearly regenerative. There was usually an inflection on the rising phase of the $[Ca^{2+}]_i$ increase, and the magnitude of the transient was relatively constant once threshold stimulation intensity was reached. This regeneration is consistent with models that propose that Ca^{2+} released from the ER acts synergistically with IP_3 to cause further release and propagating waves (Lechleiter and Clapham, 1992; Wang and Thompson, 1995). This model also may explain why spike-evoked release transients at different locations were more synchronous than release transients evoked without spikes. In this model, Ca^{2+} must diffuse from the release site to neighboring sites to combine with IP_3 at those sites to cause release. This diffusion time is responsible for much of the propagation delay of Ca^{2+} waves. However, when spikes are generated, a pulse of Ca^{2+} appears simultaneously at all locations. If there is sufficient IP_3 at those locations, release will occur without a significant delay.

Action potentials were effective in causing release within a window of <1 s following synaptic stimulation. This time is about the typical duration for a release transient in the dendrites evoked by synaptic stimulation without spikes. This similarity can be explained according to the above model if the time course of the $[Ca^{2+}]_i$ change evoked by synaptic stimulation alone also matches the time course of elevated IP_3 within the same region in the cell. If this idea is correct, then our experiments also suggest that the combined time for the synthesis and persistence of IP_3 within pyramidal neurons is <1 s.

The synergistic release of Ca^{2+} by synaptic activation and backpropagating action potentials is a second Hebbian mechanism causing $[Ca^{2+}]_i$ increases in pyramidal neurons. Previous studies have emphasized $[Ca^{2+}]_i$ increases due to Ca^{2+} entry through NMDA receptor channels enhanced by postsynaptic depolarization. Spikes also enhance these increases; the cumulative $[Ca^{2+}]_i$ increase is greater than the sum of the increase due to NMDA receptor activation alone and the increase from spike generation alone (Yuste and Denk, 1995; Koester and Sakmann, 1998; Schiller et al., 1998). The synergistic effect of spikes and mGluR stimulation is more dramatic. Since release is regenerative, a single backpropagating spike can switch the $[Ca^{2+}]_i$ increase from a level close to rest to a level of several micromolars.

The role of spikes in these Hebbian processes is interesting since backpropagating action potentials are important in the induction of some forms of long-term potentiation (LTP) and long-term depression (LTD) in pyramidal neurons (Magee and Johnston, 1997; Markram et al., 1997). Whether the interaction of spikes with NMDA receptor–mediated processes or mGluR-mediated processes (or both) is critical has yet to be determined. There is clearly a difference between the spatial distribution of the NMDA receptor–mediated $[Ca^{2+}]_i$ changes and that of the mGluR-mediated release transients we observed. These two spatially distinct $[Ca^{2+}]_i$ changes may serve different functions. The NMDA receptor–mediated changes, possibly confined to spines (Koester and Sakmann, 1998), indicate the location of the synaptic input and could reflect the synapse specificity of LTP induction. The large amplitude $[Ca^{2+}]_i$ changes due to release occur close to and sometimes include the soma. At this location, they could contribute to the activation of protein synthesis and gene expression. In addition, unlike ligand-gated or voltage-gated Ca^{2+} entry, release causes $[Ca^{2+}]_i$ increases more uniformly within the volume of the responding part of the

neuron. Therefore, these $[Ca^{2+}]_i$ changes are likely to be much higher at the nucleus and other important target locations.

Experimental Procedures

Whole-Cell Recording

Transverse hippocampal slices (300–400 μm thick) from 2- to 8-week-old Sprague-Dawley rats were prepared as previously described (Tsubokawa and Ross, 1997). Most experiments were from 3- to 4-week-old animals, but no significant differences were observed in the responses from animals of different ages. Slices were rapidly prepared with an ice-cold cutting solution consisting of (in mM): choline-Cl, 120; KCl, 3; $MgCl_2$, 8; NaH_2PO_4, 1.25; $NaHCO_3$, 26; and glucose, 10–20. Slices were then incubated for at least 1 hr in normal ACSF composed of NaCl, 124; KCl, 2.5; $CaCl_2$, 2; $MgCl_2$, 2; NaH_2PO_4, 1.25; $NaHCO_3$, 26; and glucose, 10 or 20, bubbled with a mixture of 95% O_2/5% CO_2, making the final pH 7.4.

Submerged and superfused slices were mounted on a stage rigidly bolted to an air table and were viewed with a 40× water immersion lens (Olympus) in an Olympus BX50 microscope mounted on an X–Y translation stage. Somatic whole-cell recordings were made using patch pipettes pulled from 1.5 mm outer diameter thick-walled glass tubing (1511-M, Friderick and Dimmock, Millville, NJ). Tight seals on CA1 pyramidal cell somata were made with the "blow and seal" technique using video-enhanced differential interference contrast optics to visualize the cells (Sakmann and Stuart, 1995). For most experiments, the pipette solution contained (in mM): K-gluconate, 140; NaCl, 4; Mg-ATP, 4; Na-GTP, 0.3; and HEPES, 10, pH adjusted to 7.2–7.4 with KOH. For most experiments, this solution was supplemented with 300 μM bis-fura-2 or 500 μM furaptra (Molecular Probes, Eugene, OR), except where noted. The open resistance of the pipettes was generally 4–6 MΩ. Capacitance was compensated almost fully. Synaptic stimulation was evoked with 200 μs pulses with a bipolar tungsten electrode that had one sharpened tip (WPI, model TM33B01KT) about 1 mm in front of the other. Temperature was maintained between 31° and 33°C. AP-5, CNQX, MCPG, and t-ACPD were obtained from Research Biochemicals International (Natick, MA). Ryanodine, CPA, TTX, low–molecular weight heparin, and Ruthenium Red were obtained from Sigma (St. Louis, MO). All other chemicals were obtained from Fisher Scientific (Piscataway, NJ).

In some experiments, we tested whether certain compounds (heparin, high concentrations of bis-fura-2) could block synaptically evoked Ca^{2+} release when they were included in the patch pipette. In these experiments, we used stimulation intensities at least twice as high as those normally required to evoke release. As controls for these experiments, we demonstrated release in other cells using pipettes that did not contain these compounds. These experiments were done on slices from the same animals and were performed at the end of the day, when the condition of the slices should be no better than that of the slices used for testing blockage.

$[Ca^{2+}]_i$ Measurements

Time-dependent $[Ca^{2+}]_i$ measurements from different regions of the pyramidal neuron were made as previously described (Lasser-Ross et al., 1991). Briefly, a Photometrics cooled charge-coupled device camera, operated in the frame transfer mode, was mounted on the camera port of the microscope. Custom software controlled pixel binning and readout parameters. Typical readout rates were 30 frames per second. Recordings of membrane potential changes and fluorescence intensity changes were synchronized. Fluorescence changes of both bis-fura-2 and furaptra were measured with single wavelength excitation (382 ± 10 nm) and emission >455 nm. $[Ca^{2+}]_i$ changes are expressed as $-\Delta F/F$, where F is the fluorescence intensity when the cell is at rest, and ΔF is the change in fluorescence during activity. Corrections were made for indicator bleaching during trials and background fluorescence levels. Resting membrane potential and fluorescence intensities were monitored throughout the experiments. Significant deviations from starting values not due to stimulation or agonist application terminated the experiments.

Acknowledgments

We thank Takafumi Inoue, Nechama Lasser-Ross, and Chris Leonard for comments on the manuscript and Nechama Lasser-Ross for computer programming. This work was supported by National Institutes of Health grant NS16295 and by a grant and a fellowship from the Human Frontier Science Program.

Received July 20, 1999; revised September 15, 1999.

References

Alford, S., Frenguelli, B.G., Schofield, J.G., and Collingridge, G.L. (1993). Characterization of Ca^{2+} signals induced in hippocampal CA1 neurones by the synaptic activation of NMDA receptors. J. Physiol. *469*, 693–716.

Berridge, M.J. (1998). Neuronal calcium signaling. Neuron *21*, 13–26.

Bezprozvanny, I., Watras, J., and Ehrlich, B.E. (1991). Bell-shaped calcium response curves of Ins(1,4,5)P_3- and calcium-gated channels from endoplasmic reticulum of cerebellum. Nature *251*, 751–754.

Bianchi, R., Young, S.R., and Wong, R.K.S. (1999). Group I mGluR activation causes voltage-dependent and voltage-independent Ca^{2+} increases in hippocampal pyramidal cells. J. Neurophysiol. *81*, 2903–2913.

Callaway, J.C., and Ross, W.N. (1995). Frequency-dependent propagation of sodium action potentials in dendrites of hippocampal CA1 pyramidal neurons. J. Neurophysiol. *74*, 1395–1403.

Congar, P., Leinekugel, X., Ben-Ari, Y., and Crepel, V. (1997). A long-lasting calcium-activated nonselective cationic current is generated by synaptic stimulation or exogenous activation of Group I metabotropic glutamate receptors in CA1 pyramidal neurons. J. Neurosci. *17*, 5366–5379.

Conn, P.J., and Pin, J.P. (1997). Pharmacology and function of metabotropic glutamate receptors. Annu. Rev. Pharmacol. Toxicol. *37*, 205–237.

Davies, C.H., Clarke, V.R.J., Jane, D.E., and Collingridge, G.L. (1995). Pharmacology of postsynaptic metabotropic glutamate receptors in rat hippocampal CA1 pyramidal neurons. Br. J. Pharmacol. *116*, 1859–1869.

Emptage, N., Bliss, T.V.P., and Fine, A. (1999). Single synaptic events evoke NMDA receptor–mediated release of calcium from internal stores in hippocampal dendritic spines. Neuron *22*, 115–124.

Finch, E.A., and Augustine, G.J. (1998). Local calcium signaling by inositol-1,4,5-trisphosphate in Purkinje cell dendrites. Nature *396*, 753–756.

Finch, E.A., Turner, T.J., and Goldin, S.M. (1991). Calcium as a coagonist of inositol trisphosphate-induced calcium release. Science *252*, 443–446.

Frenguelli, B.G., Potier, B., Slater, N.T., Alford, S., and Collingridge, G.L. (1993). Metabotropic glutamate receptors and calcium signaling in dendrites of hippocampal CA1 neurones. Neuropharmacology *32*, 1229–1237.

Friel, D.D., and Tsien, R.W. (1992). A caffeine and ryanodine-sensitive Ca^{2+} store in bullfrog sympathetic neurons modulates the effects of Ca^{2+} entry on $[Ca^{2+}]_i$. J. Physiol. *450*, 217–246.

Ghosh, T.K., Eis, P.S., Mullaney, J.M., Ebert, C.L., and Gill, D.L. (1988). Competitive, reversible, and potent antagonism of inositol 1,4,5-trisphosphate-activated calcium release by heparin. J. Biol. Chem. *263*, 11075–11079.

Helmchen, F., Imoto, K., and Sakmann, B. (1996). Ca^{2+} buffering and action potential–evoked Ca^{2+} signaling in dendrites of pyramidal neurons. Biophys. J. *70*, 1069–1081.

Iino, M. (1990). Biphasic Ca^{2+} dependence of inositol 1,4,5-trisphosphate-induced Ca^{2+} release in smooth muscle cells of the guinea pig taenia caeci. J. Gen. Physiol. *95*, 1103–1122.

Iino, M., and Endo, M. (1992). Calcium-dependent immediate feedback control of inositol 1,4,5-trisphosphate-induced Ca^{2+} release. Nature *360*, 76–78.

Jaffe, D.B., and Brown, T.H. (1994). Metabotropic glutamate receptor activation induces calcium waves within hippocampal dendrites. J. Neurophysiol. *72*, 471–474.

Jaffe, D.B., Johnston, D., Lasser-Ross, N., Lisman, J.E., Miyakawa, H., and Ross, W.N. (1992). The spread of Na^{+} spikes determines the pattern of dendritic Ca^{2+} entry into hippocampal neurons. Nature *357*, 244–246.

Khodakhah, K., and Armstrong, C.M. (1997). Inositol trisphosphate and ryanodine receptors share a common functional Ca^{2+} pool in cerebellar Purkinje neurons. Biophys. J. *73*, 3349–3357.

Kobayashi, S., Somlyo, A.V., and Somlyo, A.P. (1988). Heparin inhibits the inositol 1,4,5-trisphosphate-dependent, but not the independent, calcium release induced by guanine nucleotide in vascular smooth muscle. Biochem. Biophys. Res. Commun. *153*, 625–631.

Koester, H.J., and Sakmann, B. (1998). Calcium dynamics in single spines during coincident pre- and postsynaptic activity depend on relative timing of back-propagating action potentials and subthreshold excitatory postsynaptic potentials. Proc. Natl. Acad. Sci. USA *95*, 9596–9601.

Koizumi, S., Bootman, M.D., Bobanovic, L.K., Schell, M.J., Berridge, M.J., and Lipp, P. (1999). Characterization of elementary Ca^{2+} release signals in NGF-differentiated PC12 cells and hippocampal neurons. Neuron *22*, 125–137.

Konishi, M., Hollingworth, S., Harkins, A.B., and Baylor, S.M. (1991). Myoplasmic calcium transients in intact frog skeletal muscle fibers monitored with the fluorescent indicator furaptra. J. Gen. Physiol. *97*, 271–301.

Lasser-Ross, N., Miyakawa, H., Lev-Ram, V., Young, S.R., and Ross, W.N. (1991). High time resolution fluorescence imaging with a CCD camera. J. Neurosci. Methods *36*, 253–261.

Lechleiter, J.D., and Clapham, D.E. (1992). Molecular mechanisms of intracellular calcium excitability in X. laevis oocytes. Cell *69*, 283–294.

Lev-Ram, V., Miyakawa, H., Lasser-Ross, N., and Ross, W.N. (1992). Calcium transients in cerebellar Purkinje neurons evoked by intracellular stimulation. J. Neurophysiol. *68*, 1167–1177.

Linden, D.J. (1999). The return of the spike: postsynaptic action potentials and the induction of LTP and LTD. Neuron *22*, 661–666.

Llano, I., DiPolo, R., and Marty, A. (1994). Calcium-induced calcium release in cerebellar Purkinje cells. Neuron *12*, 663–673.

Lujan, R., Nusser, Z., Roberts, J.D., Shigemoto, R., and Somogyi, P. (1996). Perisynaptic location of metabotropic glutamate receptors mGluR1 and mGluR5 on dendrites and dendritic spines in the rat hippocampus. Eur. J. Neurosci. *8*, 1488–1500.

Magee, J.C., and Johnston, D. (1997). A synaptically controlled, associative signal for Hebbian plasticity in hippocampal neurons. Science *275*, 209–213.

Markram, H., Helm, P.J., and Sakmann, B. (1995). Dendritic calcium transients evoked by single back-propagating action potentials in rat neocortical neurons. J. Physiol. (Lond) *485*, 1–20.

Markram, H., Lubke, J., Frotscher, M., and Sakmann, B. (1997). Regulation of synaptic efficacy by coincidence of postsynaptic APs and EPSPs. Science *275*, 213–215.

Miyakawa, H., Ross, W.N., Jaffe, D., Callaway, J.C., Lasser-Ross, N., Lisman, J.E., and Johnston, D. (1992). Synaptically activated increases in Ca^{2+} concentration in hippocampal pyramidal cells are primarily due to voltage-gated Ca^{2+} channels. Neuron *9*, 1163–1173.

Naraghi, M. (1997). T-jump study of calcium binding kinetics of calcium chelators. Cell Calcium *22*, 255–268.

Pozzo-Miller, L.D., Petrozzino, J.J., Golarai, G., and Connor, J.A. (1996). Ca^{2+} release from internal stores induced by afferent stimulation of CA3 pyramidal neurons in hippocampal slices. J. Neurophysiol. *76*, 554–562.

Regehr, W.G., and Tank, D.W. (1990). Postsynaptic NMDA receptor–mediated calcium accumulation in hippocampal CA1 pyramidal cell dendrites. Nature *345*, 807–810.

Reyes, M., and Stanton, P.K. (1996). Induction of hippocampal long-term depression requires release of Ca^{2+} from separate presynaptic and postsynaptic intracellular stores. J. Neurosci. *16*, 5951–5960.

Rousseau, E., Smith, J.S., and Meissner, G. (1987). Ryanodine modifies conductance and gating behavior of single Ca^{2+} release channel. Amer. J. Physiol. *253*, C364–C368.

Sakmann, B., and Stuart, G. (1995). Patch-pipette recordings from the soma, dendrites, and axon of neurons in brain slices. In Single Channel Recording, Second Edition, B. Sakmann and E. Neher, eds. (New York: Plenum), pp. 199–211.

Schiller, J., Schiller, Y., and Clapham, D.E. (1998). Amplification of calcium influx into dendritic spines during associative pre- and postsynaptic activation: the role of direct calcium influx through the NMDA receptor. Nat. Neurosci. *1*, 114–118.

Seidler, N.W., Jona, I., Vegh, M., and Martonosi, A. (1989). Cyclopiazonic acid is a specific inhibitor of the Ca^{2+}-ATPase of sarcoplasmic reticulum. J. Biol. Chem. *264*, 17816–17823.

Seymour-Laurent, K.J., and Barish, M.E. (1995). Inositol 1,4,5-trisphosphate and ryanodine receptor distributions and patterns of acetylcholine- and caffeine-induced calcium release in cultured mouse hippocampal neurons. J. Neurosci. *15*, 2592–2608.

Sharp, A.H., McPherson, P.S., Dawson, T.M., Aoki, C., Campbell, K.P., and Snyder, S.H. (1993). Differential immunohistochemical localization of inositol 1,4,5-trisphosphate- and ryanodine-sensitive Ca^{2+} release channels in rat brain. J. Neurosci. *13*, 3051–3063.

Smith, S.J., Imagawa, T., Ma, J., Fill, M., Campbell, K.P., and Coronado, R. (1988). Purified ryanodine receptor from rabbit skeletal muscle is the calcium-release channel of sarcoplasmic reticulum. J. Gen. Physiol. *92*, 1–26.

Spruston, N., Schiller, Y., Stuart, G., and Sakmann, B. (1995). Activity-dependent action potential invasion and calcium influx into hippocampal CA1 dendrites. Science *268*, 297–300.

Takechi, H., Eilers, J., and Konnerth, A. (1998). A new class of synaptic response involving calcium release in dendritic spines. Nature *396*, 757–760.

Tsubokawa, H., and Ross, W.N. (1997). Muscarinic modulation of spike backpropagation in the apical dendrites of hippocampal CA1 pyramidal neurons. J. Neurosci. *17*, 5782–5791.

Turner, R.W., Meyers, D.E., Richardson, T.L., and Barker, J.L. (1991). The site for initiation of action potential discharge over the somatodendritic axis of hippocampal CA1 pyramidal neurons. J. Neurosci. *11*, 2270–2280.

Usachev, Y.M., and Thayer, S.A. (1997). All-or-none Ca^{2+} release from intracellular stores triggered by Ca^{2+} influx through voltage-gated Ca^{2+} channels in rat sensory neurons. J. Neurosci. *17*, 7404–7414.

Walton, P.D., Airey, J.A., Sutko, J.L., Beck, C.F., Mignery, G.A., Südhof, T.C., Deerinck, T.J., and Ellisman, M.H. (1991). Ryanodine and inositol trisphosphate receptors coexist in avian cerebellar Purkinje cells. J. Cell Biol. *113*, 1145–1157.

Wang, S.-H., and Thompson, S.H. (1995). Local positive feedback by calcium in the propagation of intracellular calcium waves. Biophys. J. *69*, 1683–1697.

Wang, Y., Rowan, M.J., and Anwyl, R. (1997). Induction of LTD in the dentate gyrus in vitro is NMDA receptor independent, but dependent on Ca^{2+} influx via low-voltage-activated Ca^{2+} channels and release of Ca^{2+} from intracellular stores. J. Neurophysiol. *77*, 812–825.

Yeckel, M.F., Kapur, A., and Johnston, D. (1999). Multiple forms of LTP in hippocampal CA3 neurons use a common postsynaptic mechanism. Nat. Neurosci. *2*, 625–633.

Yuste, R., and Denk, W. (1995). Dendritic spines as basic functional units of neuronal integration. Nature *375*, 682–684.